Determination of Relaxation Paths in the Manifold of Excited States of $Pt(2\text{-thpy})_2$ and $[Ru(bpy)_3]^{2+}$ by Time-Resolved Excitation and Emission

Josef Schmidt, Johann Strasser, and Hartmut Yersin*

Institut für Physikalische und Theoretische Chemie, Universität Regensburg, D-93040 Regensburg, Germany

Received May 17, 1996[⊗]

$Pt(2\text{-thpy})_2$ and $[Ru(bpy)_3]^{2+}$, studied as representatives of transition metal complexes with zero-field splittings (zfs) of the lowest triplets of several cm^{-1}, exhibit a series of generally not-well known time dependencies of emission decay properties. These are strongly determined by relatively slow spin−lattice relaxation (slr) processes. Thus, one finds emission decays for $[Ru(bpy)_3]^{2+}$ and $Pt(2\text{-thpy})_2$ of 220 and 600 ns at $T = 1.3$ K, respectively, which are in both compounds controlled by relaxation processes from the second to the lowest excited state, while the lowest state itself emits with a long decay of 230 and 110 μs, respectively. According to these distinctly different emission decay times observed for the two lowest excited states (of the same compound), it is possible to gain a more detailed insight into the properties of the different states by applying the techniques of spectrally highly resolved and time-resolved emission spectroscopy. In particular, this deeper insight results from the possibility to register high-quality low-temperature emission spectra also of the second excited state, hitherto not known. Moreover, from the temperature dependencies of the slr rates in $Pt(2\text{-thpy})_2$, it is concluded that at low temperature the *direct process of slr* dominates, while for $T > 2.3$ K the *Orbach process* becomes increasingly important. For $[Ru(bpy)_3]^{2+}$ the situation is similar, but the *Orbach process* grows in for $T > 6$ K. It is the highlight of the present investigation that the specific properties of slr can be used to study details of relaxation paths in the manifold of the electronically and vibrationally excited states by introducing—for the first time—the method of time-resolved excitation spectroscopy. In particular, it can be shown—without applying a sub-picosecond time resolution—that after a pulsed excitation the relaxations occur within the vibrational potential hypersurfaces of each triplet sublevel. A crossing between the triplet sublevels *does not* occur via excited vibrational states, but it takes place after the zero-point vibrational levels are reached. However, this selectivity of the relaxation paths is lost when a higher lying singlet is excited. Moreover, this new method provides access to a series of further excited state properties.

1. Introduction

Transition metal complexes with organic ligands have been investigated with increasing interest during the past decades, since these complexes exhibit an enormous potential for photophysical and photochemical applications,[1−12] which are often controlled by the properties of the lowest excited electronic states. Additionally, there is an extensive scientific interest in a better understanding of these compounds, because their electronic and vibronic characteristics differ largely from those found in purely organic molecules or in simple complexes with metal-centered transitions. In most investigations, these compounds were studied by usual spectroscopic methods, which normally give only broad and unresolved spectra. However, for a detailed characterization, highly resolved spectra are necessary, since otherwise important features may be smeared out and thus may be completely hidden. Moreover, the spectra usually registered display only time-integrated information, which means that essential spectral developments in time are also smeared out. Thus, an application of high-resolution and time-resolved spectroscopy to transition metal complexes makes it possible to uncover a series of significant but not yet well-known properties of the lowest excited electronic states.

Important time developments in the low-temperature emission are governed by the amount of zero-field splittings (zfs) of, for example, the lowest triplet into sublevels. The corresponding energy separations largely determine the rates of spin−lattice relaxation (slr). For instance, this process can be so slow that one specific sublevel is not populated during the emission lifetimes of the two other sublevels.[13] In a series of recent investigations of various transition metal complexes, it was shown that the zfs can be varied over a large range from about 0.1 to more than 200 cm^{-1}, depending on the admixture of metal d character to the wave functions of the lowest triplets. For instance, small zfs values of the order of 0.1 cm^{-1} (≙3 GHz), as found for most organic molecules,[14−19] are registered for the

[⊗] Abstract published in *Advance ACS Abstracts,* July 1, 1997.

(1) Lehn, J. M. *Supramolecular Chemistry*; Verlag Chemie: Weinheim, Germany, 1995.
(2) Roundhill, D. M. *Photochemistry and Photophysics of Metal Complexes*; Plenum Press: New York, 1994.
(3) Yersin, H., Ed. *Electronic and Vibronic Spectra of Transition Metal Complexes I*; Topics in Current Chemistry, Vol. 171; Springer Verlag: Berlin, 1994.
(4) Williams, A. F.; Floriani, C.; Merbach, A. E. *Perspectives in Coordination Chemistry*; Verlag Chemie: Weinheim, Germany, 1992.
(5) Kalyanasundaram, K. *Photochemistry of Polypyridine and Porphyrin Complexes*; Academic Press: London, 1992.
(6) Yersin, H., Vogler, A., Eds. *Photochemistry and Photophysics of Coordination Compounds*; Springer Verlag: Berlin, 1987.
(7) (a) O'Regan, B.; Grätzel, M. *Nature* **1991**, *353*, 737. (b) Grätzel, M. *Platinum Met. Rev.* **1994**, *38*, 151.
(8) Maestri, M.; Balzani, V.; Deuschel-Cornioley; von Zelewsky, A. *Adv. Photochem.* **1992**, *17*, 1.
(9) Kido, J.; Kimura, M.; Nagai, K. *Science* **1995**, *267*, 1332.
(10) Kritzenberger, J.; Bernhardt, G.; Gust, R.; Pistor, P.; Schönenberger, H.; Yersin, H. *Monatsh. Chem.* **1993**, *124*, 587.
(11) (a) Klimant, I.; Belser, P.; Wolfbeis, O. S. *Talanta* **1994**, *41*, 985. (b) Terpetschnig, E.; Szmacinski, H.; Malak, H.; Lakowicz, J. R. *Biophys. J.* **1995**, *68*, 342.
(12) Maede, T. J.; Kayyem, F. J. *Angew. Chem.* **1995**, *107*, 358.
(13) Donges, D.; Nagle, J. K.; Yersin, H. *Inorg. Chem.* **1997**, *36*, 3040.
(14) Tinti, D. S.; El-Sayed, M. A. *J. Chem. Phys.* **1971**, *54*, 2529.
(15) Matsuzaki, K.; Sasaki, M.; Azumi, T. *J. Chem. Phys.* **1976**, *65*, 3326.

S0020-1669(96)00565-4 CCC: $14.00

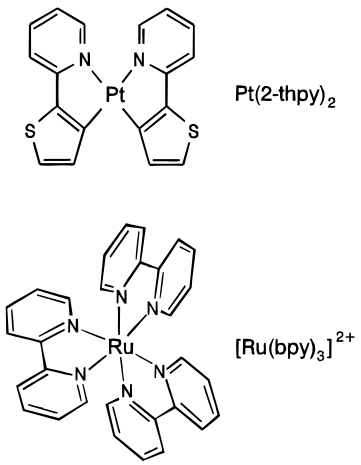

Figure 1. Structures of Pt(2-thpy)$_2$ and [Ru(bpy)$_3$]$^{2+}$, investigated in an *n*-octane Shpol'skii matrix and in a crystalline [Zn(bpy)$_3$](ClO$_4$)$_2$ matrix, respectively.

lowest triplets of transition metal complexes, if the corresponding states are mainly ligand centered. Examples are Pd(2-thpy)$_2$[20] and [Rh(bpy)$_3$]$^{3+}$ [21−24] (with 2-thpy$^-$ = the ortho-C-deprotonated form of 2-(2-thienyl)pyridine and bpy = 2,2′-bipyridine). Usually, conventional optical spectroscopy does not provide details about the properties of the triplet sublevels with such small splittings. But phosphorescence−microwave double-resonance or ODMR (optical detection of magnetic resonance) experiments can often be carried out and supply much information.[14−23] Interestingly, in a recent paper[25] we showed that by *time-resolved emission* spectroscopy individual spectra corresponding to the different triplet sublevels (split by ≈0.1 cm^{-1}) can also be well resolved although the spectral resolution (≈2 cm^{-1}) was lower by at least a factor of 20. These time-resolved spectra allowed deep insight into vibronic coupling properties and radiative deactivation paths corresponding to the individual sublevels.

On the other hand, it is expected that compounds with zfs of the order of several cm^{-1} will exhibit a series of different physical properties. In particular, different time developments will occur, since additional and relatively fast processes of slr will become important. Interestingly, an increase of zfs can be "tuned" in chemically by changing the central metal ion from Pd^{2+} to Pt^{2+} and from Rh^{3+} to Ru^{2+}. This induces an increase of metal character in the lowest triplets and thus leads to zfs of 7 and 16 cm^{-1} for Pt(2-thpy)$_2$[26] and of 8.7 and 61 cm^{-1} for [Ru(bpy)$_3$]$^{2+}$ [27−29] (Figure 1). In these situations, phosphorescence−microwave double-resonance methods are extremely difficult to apply, since high-frequency spectrometers for a 210 GHz (≙7 cm^{-1}) range, for example, are not available. Therefore, *only* optical measurements can be carried out. Fortunately, highly resolved spectra can be obtained for Pt(2-thpy)$_2$ in a Shpol'skii matrix[26] and for [Ru(bpy)$_3$]$^{2+}$ in a [Zn(bpy)$_3$](ClO$_4$)$_2$ matrix.[27−30] Thus, it is the main purpose of this contribution to investigate compounds with relatively large zfs and to study relaxation paths and times by using the methods of time-resolved emission spectroscopy. Moreover, a new technique, *time-resolved excitation spectroscopy*, will be described here for the first time. In particular, this new method provides experimental information about specific relaxation paths after excitation into individually excited vibrational states of different triplet sublevels.

2. Experimental Section

The preparation of Pt(2-thpy)$_2$[31] and the application of the Shpol'skii matrix technique[26,32] are described elsewhere. According to the final concentration of Pt(2-thpy)$_2$ in the matrix of ≈10^{-5} mol/L, the chromophores are well isolated. [Ru(bpy)$_3$](ClO$_4$)$_2$[33] and [Zn(bpy)$_3$](ClO$_4$)$_2$[27] were prepared, and doped crystals[27,29] were grown as described in the references given. The measurements were mainly performed at 1.3 K. This temperature was achieved by pumping off He in a Leybold−Heraeus BBK 100 cryostat. As excitation source a nitrogen laser (Lasertechnik Berlin MSG 210-TD, λ_{exc} = 337.1 nm, pulse width ≈ 0.5 ns, repetition rate = 100 Hz) or a Nd YAG laser (SL803 Spectron, third harmonic at 355 nm, pulse width ≈ 12 ns, repetition rate = 20 Hz) with a pumped dye laser (Lambda Physik FL 2000, modified to a spectral resolution of 0.15 cm^{-1} by Radiant Dyes) was used. To avoid sample heating, the exciting laser pulses were strongly attenuated by filters. The optical set-up for recording the spectra is described elsewhere.[34,35] Decay curves were registered with a fast multiscaler (minimum dwell time 0.5 ns/channel) combined with a multichannel data processor (7885 Multiscaler and multichannel data processor, FAST ComTec GmbH). The time-resolved spectra were recorded with a gated photon counter (Stanford Research Systems, Model SR 400).

3. Results and Discussion

3.1. Processes of Spin−Lattice Relaxation (slr). A relaxation from an excited electronic state to a second closely spaced state can be very slow, if the energy separation lies, for example, between about 0.1 and 30 cm^{-1}. Such values are often found for zero-field splittings (zfs) of spin sublevels, for instance, of triplet sublevels. According to this energy range, lattice modes (phonons) are usually involved in the relaxation processes. The phonons may be absorbed, emitted, and/or scattered due to different mechanisms. Consequently, different dependences of the relaxation rates on temperature and energy separations occur. Since these mechanisms have only rarely been discussed in connection with properties of transition metal complexes, it is useful to shortly summarize the main mechanisms:[36−48]

(16) Schweitzer, D.; Hausser, K. H.; Vogler, H.; Diederich, F.; Staab, H. A. *Mol. Phys.* **1982**, *46*, 1141.
(17) Clarke, R. H., Ed. *Triplet State ODMR Spectroscopy*; John Wiley: New York, 1982.
(18) Okabe, N.; Ikeyama, T.; Azumi, T. *Chem. Phys. Lett.* **1990**, *165*, 24.
(19) Azumi, T.; Miki, H. In *Electronic and Vibronic Spectra of Transition Metal Complexes II*; Yersin, H., Ed.; Topics in Current Chemistry, Vol. 191; Springer Verlag: Berlin, 1997; p 1.
(20) Yersin, H.; Schützenmeier, S.; Wiedenhofer, H.; von Zelewsky, A. *J. Phys. Chem.* **1993**, *97*, 13496.
(21) Komada, Y.; Yamauchi, S.; Hirota, N. *J. Phys. Chem.* **1986**, *90*, 6425.
(22) Westra, J.; Glasbeek, M. *Chem. Phys. Lett.* **1990**, *166*, 535.
(23) Westra, J.; Glasbeek, M. *Chem. Phys. Lett.* **1991**, *180*, 41.
(24) Humbs, W.; Yersin, H. *Inorg. Chem.* **1996**, *35*, 2220.
(25) Schmidt, J.; Wiedenhofer, H.; von Zelewsky, A.; Yersin, H. *J. Phys. Chem.* **1995**, *99*, 226.
(26) Wiedenhofer, H.; Schützenmeier, S.; von Zelewsky, A.; Yersin, H. *J. Phys. Chem.* **1995**, *99*, 13385.
(27) Yersin, H.; Braun, D. *Chem. Phys. Lett.* **1991**, *179*, 85.
(28) Braun, D.; Huber, P.; Wudy, J.; Schmidt, J.; Yersin, H. *J. Phys. Chem.* **1994**, *98*, 8044.
(29) Yersin, H.; Humbs, W.; Strasser, J. *Coord. Chem. Rev.* **1997**, *159*.
(30) Kato, M.; Yamauchi, S.; Hirota, N. *Chem. Phys. Lett.* **1989**, *157*, 543.
(31) Chassot, L.; von Zelewsky, A. *Inorg. Chem.* **1987**, *26*, 2814.
(32) Shpol'skii, E. V. *Sov. Phys. Usp. (Engl. Transl.)* **1960**, *3*, 372.
(33) Gallhuber, E.; Hensler, G.; Yersin, H. *Chem. Phys. Lett.* **1985**, *120*, 445.
(34) Stock, M.; Yersin, H. *Chem. Phys. Lett.* **1976**, *40*, 423.
(35) Yersin, H.; Gliemann, G. *Messtechnik (Braunschweig)* **1972**, *80*, 99.
(36) VanVleck, J. H. *Phys. Rev.* **1940**, *57*, 426.
(37) Orbach, R. *Proc. R. Soc. (London)* **1961**, *A264*, 456.
(38) Scott, P. L.; Jeffries, C. D. *Phys. Rev.* **1962**, *127*, 32.
(39) Geschwind, S.; Devlin, G. E.; Cohen, R. L.; Chinn, S. R. *Phys. Rev.* **1965**, *137A*, 1087.
(40) Manenkov, A. A., Orbach, R. Eds. *Spin−Lattice Relaxation in Ionic Solids*; Harper and Row Publishers: New York, 1966.
(41) (a) Abragam, A.; Bleaney, B. *Electron Paramagnetic Resonance of Transition Ions*; Clarendon Press: Oxford, U.K., 1970; Chapter 10, p 541. (b) Walker, M. B. *Can. J. Phys.* **1968**, *46*, 1347.
(42) Konzelmann, U.; Kilpper, D.; Schwoerer, M. *Z. Naturforsch.* **1975**, *30A*, 754.

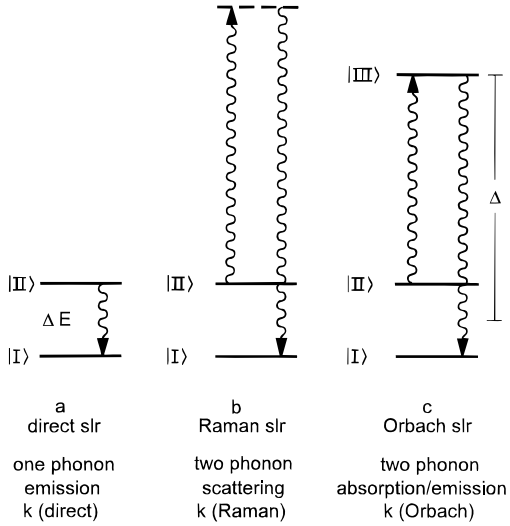

Figure 2. Important mechanisms of spin−lattice relaxation (slr). |I⟩, |II⟩, and |III⟩ represent electronic states of a molecule. *k* is the rate of slr, and Δ is the average energy separation between states |I⟩, |II⟩ and |III⟩.

Direct Process of slr. Figure 2a shows two electronic states |I⟩ and |II⟩ with an energy separation ΔE of a molecule in a lattice environment. It is assumed that state |II⟩ is populated either by a relaxation from a higher lying state, for example, by an intersystem crossing process, or by an excitation of just that electronic state. A relaxation from |II⟩ to |I⟩ may occur by an emission of one phonon having the energy ΔE. This process is called *direct slr*. The corresponding rate *k* (direct) can be expressed as (e.g., see refs 41 and 45)

$$k(\text{direct}) = \text{constant} \times (\Delta E)^3 v^{-5} \langle \text{II}|H_1|\text{I}\rangle|^2 \coth(\Delta E/2k_B T) \quad (1)$$

where v is the mean velocity of sound in the lattice, k_B is the Boltzmann constant, and the matrix element describes the coupling of the two states by the electron-spin−phonon interaction operator H_1. At low temperature ($\Delta E \gg k_B T$), coth(ΔE/$2k_B T$) may be approximated by 1. Thus, one obtains the well-known $(\Delta E)^3$ dependence for *k* (direct). Indeed, in several experimental investigations,[41−43] a corresponding dependence of the slr *time* T_1 (direct) $= k^{-1}$ (direct) on $(\Delta E)^{-3}$ is found at low temperature ($T < 2$ K) and for ΔE values of the order of several cm^{-1}. For Pt(2-thpy)$_2$ and [Ru(bpy)$_3$]$^{2+}$ discussed in the present investigation, this process of direct slr will also be of great importance. (See sections 3.2.2 and 3.3.1 and ref 49.) For completeness, it is mentioned that for $\Delta E \lesssim k_B T$, *k* (direct) is roughly proportional to $(\Delta E)^2 T$. (See, for example, refs 47 and 48.) Thus it follows that, for compounds with zfs of the triplet sublevels of the order of 0.1 cm^{-1}, *k* (direct) is often very small at low temperature (e.g., at $T = 1.3$ K) and may be neglected compared to radiative and nonradiative decays to the ground state. Consequently, the different sublevels emit independently.[13−25]

Raman Process of slr. In addition to the one-phonon process described above, a two-phonon scattering process according to Figure 2b can also occur. The temperature dependence of this Raman process of slr can be approximated (for the non-Kramers situation) at low temperature and for $\Delta E \ll$ phonon energies to *k*(Raman) $\sim T^7$ [38,41a,45] or to *k*(Raman) $\sim T^5$.[41a,b] Also these processes have been observed experimentally.[38,41a,b,47,48] At very low temperature and in the presence of a fast direct process, the Raman scattering can usually be neglected.

Orbach Process of slr. When a real state |III⟩ lies above the states |I⟩ and |II⟩ within the energy range of phonons, one phonon may be absorbed, while a second phonon can be emitted from this state |III⟩ (Figure 2c). This process of slr, called the Orbach process, can be described by resonant upward and downward direct processes. The corresponding rate can roughly be approximated to[37,38,40,41a,45]

$$k(\text{Orbach}) = \text{constant} \times \Delta^3 v^{-5} \exp(-\Delta/k_B T) \quad (2)$$

where Δ represents the mean energy separation between the states |I⟩, |II⟩ and state |III⟩. The importance of the Orbach process has often been demonstrated.[37−41a,44−46] Recently, it could be shown that this process also governs the slr in [Ru(bpy)$_3$]$^{2+}$ for $T \gtrsim 6$ K.[50] (See also Figure 5.)

For completeness, it is mentioned that in general all three processes have to be taken into account and may vary in importance in different temperature ranges.

3.2. Pt(2-thpy)$_2$. Pt(2-thpy)$_2$ is a representative of a new class of ortho-metalated compounds. Its photophysical and photochemical properties have been investigated in a series of recent publications.[8,26,31,51−60] Several of these studies focused on the characterization of the lowest excited and emitting triplet states,[26,51,52,55−57,60] which were assigned as ligand-centered with an appreciable amount of metal-to-ligand charge transfer (MLCT) character.[26,60] Properties of the lowest triplet will be discussed hereafter.

3.2.1. Triplet Sublevels and Time-Integrated Emission. Sharp-line phosphorescence and triplet excitation spectra were recently obtained at low temperatures, when Pt(2-thpy)$_2$ was dissolved in an *n*-octane Shpol'skii matrix.[26] The dominant site exhibits three triplet sublevels |I⟩, |II⟩, and |III⟩, zero-field split by 16 cm^{-1}. (See the energy level diagram in Figure 3; the decay properties are explained in section 3.2.2.) It was found that the transition between the lowest sublevel |I⟩ and the electronic ground state |0⟩ at 17 156 cm^{-1} is strongly forbidden. Thus, the electronic origin is extremely weak. However, a careful inspection of the usual time-integrated emission spectrum measured at $T = 1.3$ K (Figure 4a, inset) allows us to identify this transition. The emission spectrum (Figure 4a) shows a

(43) Renk, K. F.; Sixl, H.; Wolfrum, H. *Chem. Phys. Lett.* **1977**, *52*, 98.
(44) Broer, M. M.; Hegarty, J.; Imbusch, G. F.; Yen, W. M. *Opt. Lett.* **1978**, *3*, 175.
(45) Henderson, B.; Imbusch, G. F. *Optical Spcetroscopy of Inorganic Solids*; Oxford Science Publications, Clarendon Press: Oxford, U.K., 1989; p 228.
(46) Schmidt, J. In *Relaxation Processes in Molecular Excited States*; Fünfschilling, J., Ed.; Kluwer Academic Publishers: Dordrecht, The Netherlands, 1989; p 3.
(47) Wolfe, J. P. *Chem. Phys. Lett.* **1971**, *10*, 212.
(48) Hall, L. H.; El-Sayed, M. A. *Chem. Phys.* **1975**, *8*, 272.
(49) Yersin, H.; Braun, D. *Coord. Chem. Rev.* **1991**, *111*, 39.
(50) Yersin, H.; Strasser, J. *J. Lumin.* **1997**, *72−74*, 462.
(51) Balzani, V.; Maestri, M.; Melandri, A.; Sandrini, D.; Chassot, L.; Cornioley-Deuschel, C.; Jolliet, P.; Maeder, U.; von Zelewsky, A. In *Photochemistry and Photophysics of Coordination Compounds*; Yersin, H., Vogler, A., Eds.; Springer Verlag: Berlin, 1987; p 71.
(52) Maestri, M.; Sandrini, D.; Balzani, V.; von Zelewsky, A.; Jolliet, P. *Helv. Chim. Acta* **1988**, *71*, 134.
(53) Sandrini, D.; Maestri, M.; Balzani, V.; Chassot, L.; von Zelewsky, A. *J. Am. Chem. Soc.* **1987**, *109*, 7720.
(54) Bonafede, S.; Ciano, M.; Bolletta, F.; Balzani, V.; Chassot, L.; von Zelewsky, A. *J. Phys. Chem.* **1986**, *90*, 3836.
(55) Sandrini, D.; Maestri, M.; Ciano, M.; Balzani, V.; Lueoend, R.; Deuschel-Cornioley, C.; Chassot, L.; von Zelewsky, A. *Gazz. Chim. Ital.* **1988**, *118*, 661.
(56) Schützenmeier, S. Thesis, Universität Regensburg, 1992.
(57) Wiedenhofer, H. Thesis, Universität Regensburg, 1994.
(58) Kvam, P.-I.; Puszyk, M. V.; Cotlyr, V. S.; Balashev, K. P.; Songstad, J. *Acta Chem. Scand.* **1995**, *49*, 645.
(59) Breu, J.; Range, K.-J.; von Zelewsky, A.; Yersin, H. *Acta Crystallogr.* **1997**, *C53*, 562.
(60) Yersin, H.; Huber, P.; Wiedenhofer, H. *Coord. Chem. Rev.* **1994**, *132*, 35.

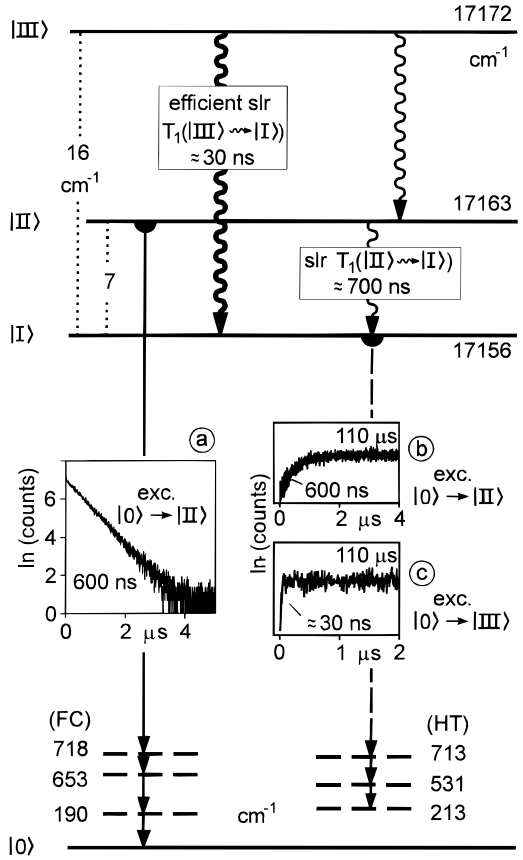

Figure 3. Energy level diagram and spin−lattice relaxation properties for the three triplet sublevels of Pt(2-thpy)$_2$ in *n*-octane (dominant site) at $T = 1.3$ K. The transition from state |I⟩ to the ground state |0⟩ is strongly forbidden, and the corresponding decay time is $\tau_I = 110$ μs.[26] The emission from state |II⟩ cannot be frozen out even at $T = 1.3$ K, due to the relatively slow slr from state |II⟩ to state |I⟩. One observes a 600 ns emission decay from state |II⟩. An excitation at the electronic origin II (|0⟩ → |II⟩) is followed by a 600 ns decay, when measured at the 190, 653, or 718 cm^{-1} vibrational satellite to origin II (inset a), and by a 600 ns rise, when measured at the 231 or 531 cm^{-1} satellite to origin I (inset b). An excitation at the electronic origin III (|0⟩ → |III⟩) results in a fast rise of ≈30 ns (rough estimate) of the emission from state |I⟩ (inset c). Vibrational FC modes represent Franck−Condon-active modes while HT modes correspond to Herzberg−Teller activity.

further important result. Each prominent vibrational satellite carries more intensity than the origin I (transition |I⟩ ↔ |0⟩). Consequently, the corresponding vibrations are Herzberg−Teller (HT) active,[61−63] as has been concluded in a recent and detailed study.[26] These vibrations open the main radiative deactivation paths from |I⟩ by vibronic coupling processes. Prominent examples are the 213, 531, 713, and the 1293 cm^{-1} satellites.

The transitions from the sublevels |II⟩ and |III⟩ to the electronic ground state are much more allowed due to direct spin−orbit coupling to a higher lying singlet (see ref 26). Therefore, temperature increase, for example to $T = 20$ K, which leads to a relatively fast thermal equilibration between the three sublevels, results in an emission mainly from these two states. Thus, one obtains a "doublet" structure in the emission spectrum, displaying an energy separation of 9 cm^{-1} between |II⟩ and |III⟩ (Figure 4d). Due to the relatively high allowedness of the electronic transitions |III⟩, |II⟩ → |0⟩, Herzberg−Teller coupling does not play an important role (compare refs 20, 25, 26, and 61−63). The large number of vibrational satellites, having weak intensities compared to the transition at the origin II, are mostly assigned to vibrational modes of Franck−Condon (FC) activiy.[26] Typical representatives are the 190, 653, 718, and 1123 cm^{-1} satellites. In the scope of the present investigation, it is important that most of these FC-active vibrational modes observed in emission and accompanying the transitions |III⟩, |II⟩ → |0⟩ have vibrational energies different from those of the HT-active modes being observed in the emission from |I⟩. Thus, the time-integrated emission spectrum changes completely with temperature increase from 1.3 to 20 K (compare Figure 4a to Figure 4d).

3.2.2. Time-Resolved Emission and Spin−Lattice Relaxation. The emission measured in the spectral region of both electronic origins I and II shows at $T = 1.3$ K a biexponential decay with a fast component of 600 ± 10 ns and a slow one of 110 ± 5 μs (when, for example, the singlet S_1 is excited).[56,57] Such a behavior is expected if the emission arises from two different electronic states that are not in a fast equilibrium. To study this property in more detail, time-resolved emission spectra were recorded at 1.3 K, using a nitrogen laser as excitation source. Figure 4c shows the emission detected immediately after the exciting pulse (delay $t = 0$ ns) and integrated during a time window of $\Delta t = 500$ ns (fast emission), while Figure 4b reproduces the spectrum measured with a delay of $t = 10$ μs after the exciting pulse and integrated over a window of $\Delta t =$ 60 μs (slow emission).

The time-resolved spectra registered are found to be completely different. The slow emission (Figure 4b) exhibits (nearly) the same structure as the time-integrated emission at $T = 1.3$ K (Figure 4a). Therefore, it can be concluded that the slow-emission spectrum largely represents the emission from the lowest triplet sublevel |I⟩. (See footnote 64.) The fast-emission spectrum (Figure 4c) recorded immediately after the excitation pulse exhibits the same structure as the time-integrated spectrum measured at $T = 20$ K (Figure 4d) if the emission from state |III⟩ (9 cm^{-1} higher lying peaks of the "doublet" structure) is disregarded. An emission from this state |III⟩ is not observed at $T = 1.3$ K due to the very fast process of slr that depletes state |III⟩ efficiently (see below). Consequently, the fast-emission spectrum corresponds mainly to the emission from state |II⟩ when the thermal equilibrium is not yet reached.

These time developments are understood on the basis of a slr from state |II⟩ to state |I⟩, which occurs with the slr time T_1. $T_1 = k_{slr}^{-1}$ is slightly different from the experimentally determined decay time of $k_{exp}^{-1} = 600$ ns at $T = 1.3$ K, since the usual emission lifetime $\tau_{II} = (k_r + k_{nr})^{-1}$ of state |II⟩ must also be taken into account. k_r and k_{nr} are the radiative and the nonradiative decay rates for the processes from the excited state |II⟩ to the ground state |0⟩. In ref 57, τ_{II} is estimated to be ≈4 μs (from the temperature dependence of the long emission lifetime component). Consequently, the depletion of state |II⟩ is given by the processes of slr and radiative and nonradiative decays to the ground state. Taking the corresponding rates, one obtains

$$T_1 = (k_{exp} - 1/\tau_{II})^{-1} \approx 700 \text{ ns} \qquad (3)$$

This process of the relatively slow slr of 700 ns can further be investigated by selectively exciting state |II⟩ with a pulsed laser. Thus, an initial population of state |I⟩ is prevented, which usually would occur after an excitation into a higher lying singlet (see also below). In contrast to the situation found for most organic

(61) Albrecht, A. C. *J. Chem. Phys.* **1963**, *38*, 354.
(62) Hochstrasser, R. M. *Molecular Aspects of Symmetry*; W. A. Benjamin Inc.: New York, 1966.
(63) Gastilovich, E. A. *Sov. Phys. Usp.* **1991**, *34*, 592.
(64) The occurrence of the electronic origin II in the slow spectrum is not expected (Figure 4b); its appearance is simply a consequence of a residual thermal repopulation of state |II⟩ (even at $T = 1.3$ K) and of its relatively high radiative rate to |0⟩.
(65) Donges, D. Ph.D. Thesis, Universität Regensburg, 1997.

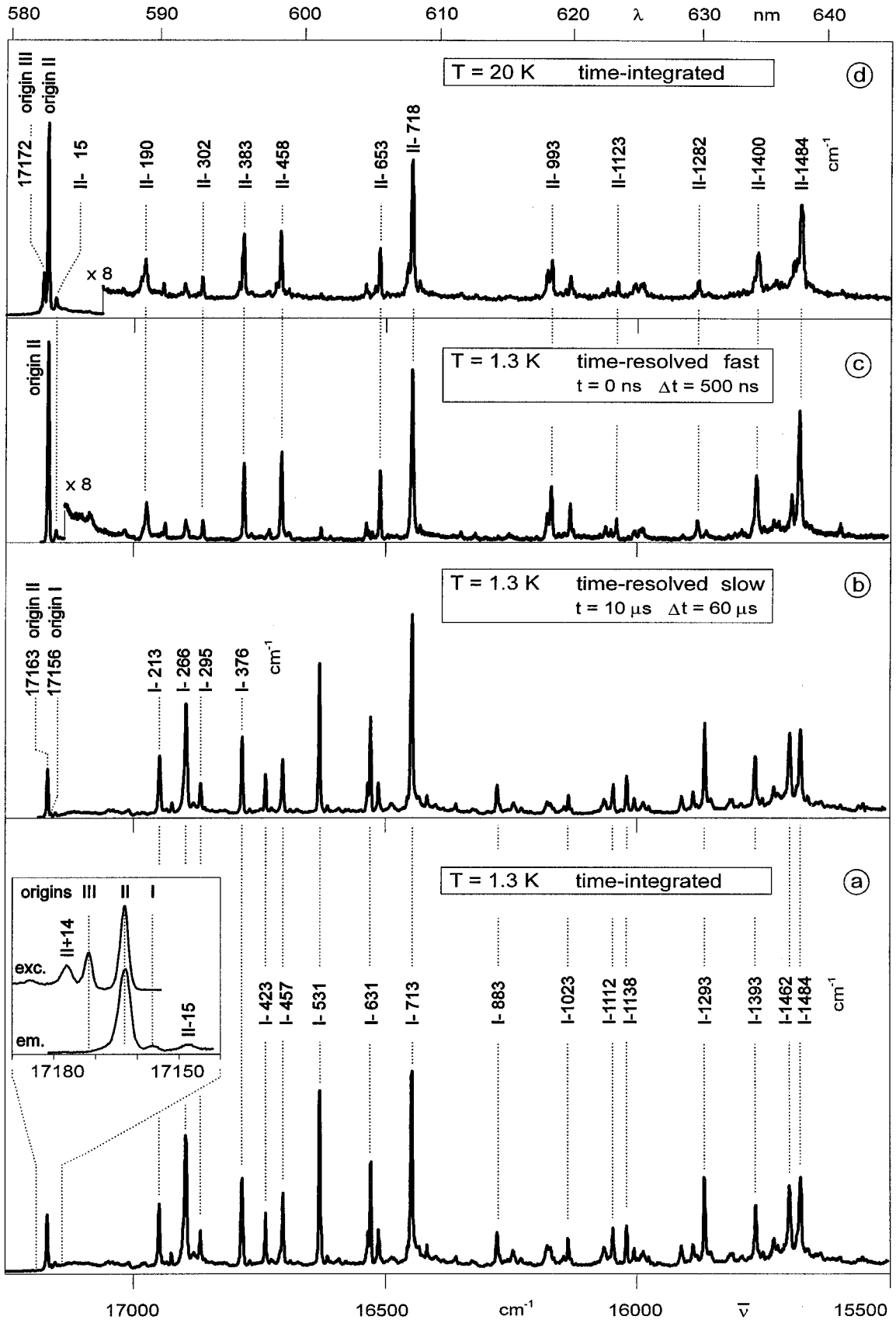

Figure 4. Emission spectra of Pt(2-thpy)$_2$ in an *n*-octane Shpol'skii matrix. The excitation energy is chosen to excite a higher lying singlet. Thus, one obtains an initial population of all three triplet sublevels. (λ_{exc} = 337.1 nm). (a) Time-integrated emission at T = 1.3 K (from ref 26). The inset shows the region of the electronic origins in emission and excitation and demonstrates the weakness of the transition $|I\rangle \leftrightarrow |0\rangle$ (origin I). (b) Time-resolved emission (slow): delay time t = 10 μs, time window Δt = 60 μs. (c) Time-resolved emission (fast): delay time t = 0 ns, time window Δt = 500 ns. (d) Time-integrated emission at T = 20 K (from ref 26). The energies of the vibrational satellites are given in cm^{-1} relative to the corresponding origins I and II, respectively.

molecules, such an experiment is possible with transition metal complexes, since spin−orbit coupling to the triplet sublevels—induced by the metal—can supply appreciable allowedness to the singlet−triplet transitions. For Pt(2-thpy)$_2$, the transitions $|0\rangle \rightarrow |II\rangle$, $|III\rangle$ show an absorption, while $|0\rangle \rightarrow |I\rangle$ is strongly forbidden (see section 3.2.1 and ref 26). After

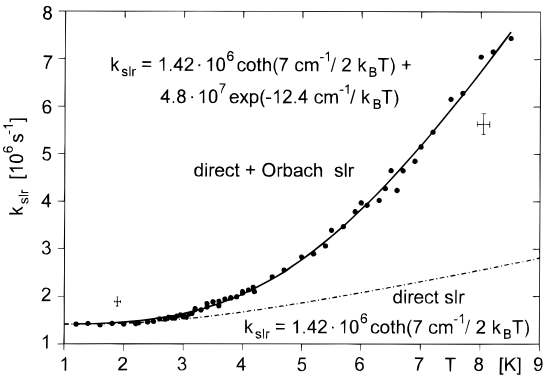

Figure 5. Spin−lattice relaxation (slr) rate k_{slr} of Pt(2-thpy)$_2$ in an *n*-octane Shpol'skii matrix versus temperature for the relaxation process $|II\rangle \rightarrow |I\rangle$. The corresponding emission is detected at the origin line II (17 163 cm^{-1}). In the temperature range (1.2 K $\leq T \leq$ 2.5 K) the spin−lattice relaxation is dominated by the direct process, while at higher temperature the Orbach process strongly grows in. The experimental data are fitted by the expression given in the figure (solid line). For comparison, the calculated temperature dependence of the direct process alone is also shown (dash−dot curve).

selective excitation of state $|II\rangle$, it is of interest to observe the time evolution of the emission from $|I\rangle$ compared to the decay from $|II\rangle$. For this experiment, one must make a proper choice of the detection energy. This is seen upon inspecting the time-resolved emission spectra (Figures 4b,c). They exhibit the very interesting features that the vibrational satellites at 531 and 713 cm^{-1} (for example) belong *selectively* to the emitting state $|I\rangle$, while the 653 and 718 cm^{-1} satellites (for example) are *selectively* connected with state $|II\rangle$ (see refs 25 and 26). Consequently, after an excitation of $|0\rangle \rightarrow |II\rangle$, the evolution of the emission measured at the 531 cm^{-1} satellite (to $|I\rangle \rightarrow |0\rangle$) should exhibit a growing in with a rise time of ≈600 ns and a subsequent decay with the usual emission lifetime of $|I\rangle$ (τ_I = 110 μs) at T = 1.3 K, while the emission measured at the 653 or 718 cm^{-1} satellite (to $|II\rangle \rightarrow |0\rangle$) should decay immediately with the ≈600 ns component. Indeed, this behavior is found, as is demonstrated in Figure 3 (insets a and b).

An equivalent experiment but exciting state $|III\rangle$ should also be possible. However, according to the $(\Delta E)^{-3}$ dependence of the slr time T_1 for direct processes (eq 1), the slr from state $|III\rangle$ to state $|I\rangle$ should be faster by a factor of about 12 (from (16 cm^{-1}/7 cm^{-1})^3) than the slr from state $|II\rangle$ to state $|I\rangle$. Indeed, the experiment shows after a pulsed excitation into state $|III\rangle$ a rise of the emission from state $|I\rangle$ (Figure 3, inset c). The corresponding rise time can be roughly estimated to be 30 ± 10 ns. This value is by a factor of 2 smaller than expected (from 700 ns/12 ≈ 60 ns). Presumably, this is an indication of somewhat different matrix elements of electron−phonon interactions (see eq 1) for both situations.

Moreover, it is found that the intensity of the short-lived emission component from state $|II\rangle$ (decaying by 600 ns) is larger by a factor of about 10 when state $|II\rangle$ itself is excited compared to an excitation of state $|III\rangle$, whereas the ratio of transition probabilities[26] for the transitions $|0\rangle \rightarrow |II\rangle$ to $|0\rangle \rightarrow |III\rangle$ is only 1.6. This behavior is also a consequence of the more efficient relaxation from state $|III\rangle$ to state $|I\rangle$ compared to the relaxation from $|III\rangle$ to $|II\rangle$ (Figure 3). This property will allow us to determine specific relaxation paths involving different triplet sublevels, as discussed in the next section.

A determination of the relevant mechanism(s) of slr is possible if the fast-decay component is investigated as function of temperature. Figure 5 shows that the rate $k_{slr} = k_{exp} - 1/\tau_{II}$ is nearly constant in the temperature range from 1.3 to ≈2.3 K but exhibits a steep rise with further temperature increase. (In a very good approximation, τ_{II} is independent of temperature.) According to section 3.1, this behavior can be explained by a *direct* process of slr in the low-temperature range *and* by an additional *Orbach* process for higher temperatures. The latter process is expected to be more efficient than the Raman process due to the occurrence of an electronic state $|III\rangle$ being only several cm^{-1} above $|II\rangle$ (Figure 3). Indeed, the experimental results can be well described by the direct and the Orbach processes:

$$k_{slr}(T) = A \coth(\Delta E/2k_BT) + B \exp(-\Delta/k_BT) \qquad (4)$$

The best fit is obtained with the values $A = (1.42 \pm 0.1) \times 10^6$ s^{-1}, $\Delta E = 7 \pm 0.4$ cm^{-1}, $\Delta = 12.4 \pm 1$ cm^{-1}, and B = (4.8 ± 0.8) × 10^7 s^{-1}. A^{-1} gives exactly the slr time T_1 at low temperature, ΔE is just the energy separation measured between states $|I\rangle$ and $|II\rangle$, and Δ corresponds to the average energy separation between states $|III\rangle - |II\rangle$ and $|III\rangle - |I\rangle$, as discussed in section 3.1. Usually, the value of B is much larger than the one of A (see refs 37−41a), but a comparison to an independent observable for Pt(2-thpy)$_2$ is not yet possible. For completeness it is mentioned that the slr according to the direct process alone or to both direct and Raman mechanisms does not fit the experimental data. Moreover, inclusion of the Raman process in eq 4 does not improve the fit. Therefore, it is concluded that the Raman process is not very important in the temperature range studied.

3.2.3. Time-Resolved Excitation Spectra and Relaxation Paths. In the preceding section it was shown that after a pulsed excitation at the energies of the electronic origins II and III, respectively, one finds specific emission decay properties which are characteristic of the individual triplet sublevels though an emission of state $|III\rangle$ itself is not observed at T = 1.3 K. This is possible due to the distinctly different rates and efficiences of spin−lattice relaxation. An important requirement for the observation of these characteristics is the adequate choice of vibrational satellites used for the dectection of emission. From these results a very interesting question arises as to whether the *excited vibrational* states belonging to the different *excited electronic* states $|II\rangle$ and $|III\rangle$, respectively, exhibit the same decay characteristics as found for the electronic origins. If so, one can conclude that the relaxation path occurs *within* the potential hypersurface corresponding to the individual electronic triplet sublevel. If not, it follows that an intersystem crossing between the sublevels via excited vibrational states occurs. Figure 6 illustrates this point. An answer to this important question has—to our knowledge—not yet been given. Interestingly, this will be possible by using the new method of time-resolved excitation spectroscopy—or more exactly the method of excitation spectroscopy with time-resolved detection.

As outlined in section 3.2.2, an excitation of origin III is followed by a relaxation process, which has a higher efficiency to state $|I\rangle$ (with its lifetime of τ_I = 110 μs) compared to state $|II\rangle$ (decaying with 600 ns). Moreover, the emission intensities from the two states $|I\rangle$ and $|II\rangle$, respectively, depend strongly on the vibrational satellites selected for detection. For a suitably planned measurement of time-resolved excitation spectra, one should find a spectral position for detection at which vibrational satellites corresponding to states $|I\rangle$ and $|II\rangle$ overlap. In this case, it is possible to detect the emission from both states in the same counting cycle after the laser shot. Since the spectra are averaged over a large number of such cycles (≈200 times), the spectra corresponding to different time ranges are always intrinsically normalized. An inspection of Figure 4b and Figure 4c shows that the satellites 713 cm^{-1} to origin I and 718 cm^{-1} to origin II may be registered simultaneously if the detection energy is chosen to lie within 16 443 and 16 445 cm^{-1} (Figure 6). (Similarly, this condition for detection would be fulfilled for the II-383 and the I-376 cm^{-1} satellites.) Indeed, Figure 7

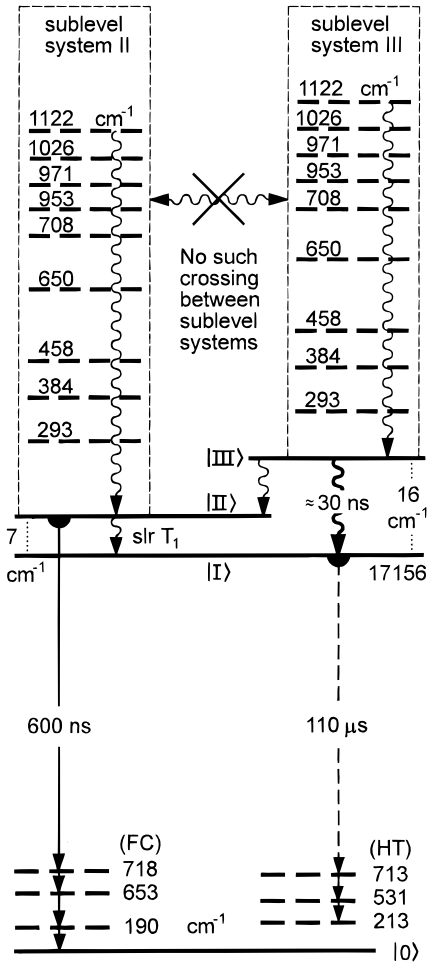

Figure 6. Triplet sublevel systems of states |II⟩ and |III⟩ of Pt(2-thpy)$_2$. By time-resolved excitation spectroscopy, it is demonstrated that an inter-sublevel system crossing does not occur via excited vibrational states but occurs only after a relaxation to the zero-point vibrational level of the respective states |II⟩ and |III⟩. Only several representative vibrational energies of a large number of vibrational modes are given.

shows that the time-resolved excitation spectra detected at the representative I-713 *and* II-718 cm^{-1} satellites exhibit significant differences. The spectrum measured with a time delay of $t =$ 10 μs and a time window of $\Delta t = 250$ μs (slow spectrum, emission from state |I⟩, Figure 7b) exhibits an electronic origin III ($|0\rangle \rightarrow |III\rangle$) being about 2.2 times more intense than that found in the fast-decaying excitation spectrum (emission from state |II⟩, time delay $t = 0$ μs, time window $\Delta t = 2$ μs, Figure 7a) for the same electronic origin III. (The intensities are normalized to the ones of origin II.)

It is an important result (displayed in Figure 7a,b) that *all vibrational satellites* of origin III up to about 1500 cm^{-1} (total range of our measurements, but only the range up to ≈720 cm^{-1} is reproduced), including phonon satellites, exhibit an intensity ratio of 2.2 ± 0.2 when the (normalized) slow component is related to the fast one. The largest deviations do not exceed the experimental error of about 10%. Thus, one finds the same intensity ratio as is determined for the electronic origin III registered in the two time-resolved spectra. This result allows us to relate the excited state vibrations to their electronic states by means of the time dependences of their intensities. Thus, it can be concluded that the relaxation from an excited vibrational state occurs by a very fast process within the individual potential hypersurface of each triplet sublevel to its zero-point vibrational level. Subsequently, a comparatively slow slr and/or emission occurs from that electronic state. This behavior corresponds exactly to what is expected for such relaxation paths.

If, on the other hand, the vibrational relaxation does not occur mainly inside the potential hypersurface of the individual triplet sublevel but makes an inter-sublevel system crossing involving a specific vibrational state, the intensity ratio for that specific vibrational satellite and presumably for all higher lying ones would distinctly differ from the ratio found for the electronic origins when the different time-resolved spectra are compared. However, this is in contrast to the experimental observation displayed in Figure 7.

For completeness, the time-resolved excitation spectra of a different, *higher* lying electronic state were also measured. In this case, one would not expect to observe any specific time dependence of the vibrational satellite structures, since these *vibrations* would certainly not interact selectively with a specific potential hypersurface of a lower lying triplet sublevel. Indeed, this is demonstrated in Figure 8. Presumably, the peak at 20 430 cm^{-1} is an origin of an MLCT transition of Pt(2-thpy)$_2$, and the structure at higher energies seems to consist of a vibrational progression which is superimposed by a number of other vibrational satellites. None of these *vibrational* satellites shows any selectivity with respect to a relaxation into one of the three triplet sublevels.

3.3. [Ru(bpy)$_3$]$^{2+}$. The lower excited states of [Ru(bpy)$_3$]$^{2+}$ result from Ru 4d−bpy π^* MLCT transitions. In particular, the three lowest excited states |I⟩, |II⟩, and |III⟩ represent sublevels of an ^{3}MLCT state, split by 8.7 and 61 cm^{-1} for [Ru(bpy)$_3$]$^{2+}$ doped into a [Zn(bpy)$_3$](ClO$_4$)$_2$ matrix. (See Figure 9. The decay properties are explained in section 3.3.1.) The properties of these states have been discussed in the scope of three different models. Two of these favor a localization of the excitation on one ligand. In the first model (i) it is assumed that a relatively strong distortion (order of 10^3 cm^{-1}) is required for a localization (e.g., see refs 66 and 67), while in the second model (ii) an extremely weak distortion (order of 0.1 cm^{-1}) is sufficient to localize the excitation on one (Ru−bpy) subunit (e.g., see ref 68). Thus, both models cannot equally be valid. On the other hand, the third model (iii) describes the excited state properties in a delocalized description. In recent reviews,[29,69] these models were carefully compared and it was demonstrated that both localization models are not valid for [Ru(bpy)$_3$]$^{2+}$ doped into [Zn(bpy)$_3$](ClO$_4$)$_2$. On the one hand, the distortion predicted by model i should lead to spectral appearances which do not occur (e.g., distinct vibrational Franck−Condon progressions[27,29,49,69] and specific vibronic structures due to partial deuteration[28,29,69]). And on the other hand, several experimental findings[68] which represent the crucial basis of model ii are not related to isolated [Ru(bpy)$_3$]$^{2+}$ complexes but result from a formation of [Ru(bpy)$_3$]$^{2+}$ clusters (compare refs 29, 69, 70, and 71). However, as presented in ref 29 one can safely assume the validity of model iii. This means that the three lowest excited states of [Ru(bpy)$_3$]$^{2+}$ doped into the rigid [Zn(bpy)$_3$](ClO$_4$)$_2$ matrix must be characterized in a delocalized description. (Compare also ref 72.)

3.3.1. Emission Decays and Spin−Lattice Relaxation. In this investigation, we are mainly interested in the time evolutions after an excitation pulse. Half a decade ago it was found,[49] by measuring the emission decay and time-resolved emission spectra in the region of the electronic origins, that the low-temperature emission ($T = 1.3$ K) displays a slr time $T_1 = 220$ ± 10 ns[73] from state |II⟩ to |I⟩, while the usual emission lifetime

(66) Kober, E. M.; Meyer, T. J. *Inorg. Chem.* **1984**, *23*, 3877.
(67) Krausz, E.; Ferguson, J. *Prog. Inorg. Chem.* **1989**, *37*, 293.
(68) Riesen, H.; Krausz, E. *J. Chem. Phys.* **1993**, *99*, 7614.
(69) Yersin, H.; Humbs, W.; Strasser, J. In *Electronic and Vibronic Spectra of Transition Metal Complexes II*; Yersin, H., Ed.; Topics in Current Chemistry, Vol. 191; Springer Verlag: Berlin, 1997; p 153.
(70) Masuda, Y.; Yamatera, H. *Bull. Chem. Soc. Jpn.* **1984**, *57*, 58.
(71) Kumar, C. V.; Williams, Z. J. *J. Phys. Chem.* **1995**, *99*, 17632.
(72) Huber, P.; Yersin, H. *J. Phys. Chem.* **1993**, *97*, 12707.

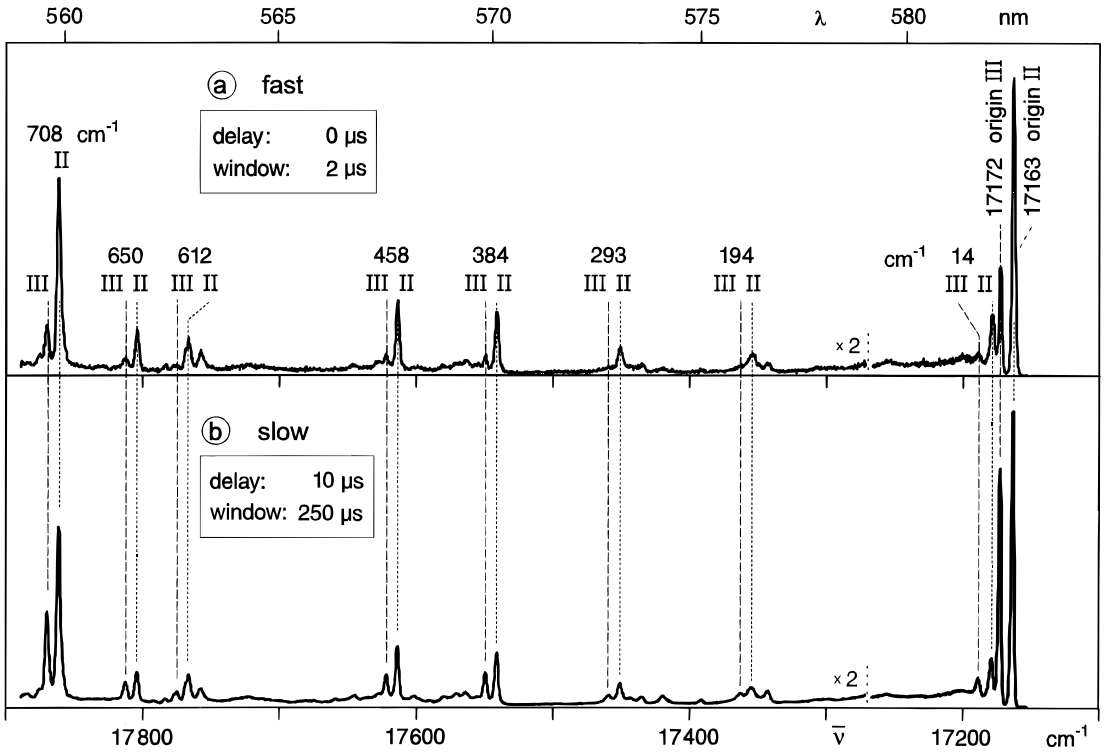

Figure 7. Time-resolved excitation spectra of Pt(2-thpy)$_2$ in an *n*-octane Shpol'skii matrix ($T = 1.3$ K): (a) time-resolved detection (of the emission) with a delay time of $t = 0$ μs and a time window of $\Delta t = 2$ μs; (b) time-resolved detection with $t = 10$ μs and $\Delta t = 250$ μs. The emission is detected selectively at $\bar{\nu}_{det} = 16\,444$ cm^{-1} with a spectral bandwidth of $\approx$3 cm^{-1}, which allows us to register simultaneously the vibrational satellites I-713 cm^{-1} and II-718 cm^{-1} (see Figure 6). The spectra are normalized to the origin II peaks. For clarity, the spectra are only reproduced up to $\approx$720 cm^{-1} from the electronic origins, but the same intensity ratio is also observed for higher lying vibrational satellites. For example, well-resolved peaks are found at 953, 971, 1026, and 1122 cm^{-1}.

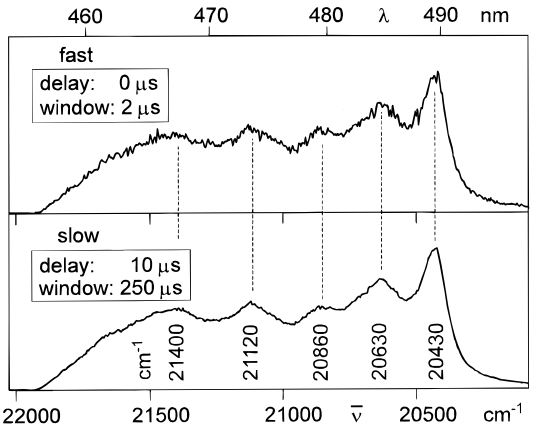

Figure 8. Time-resolved excitation spectra of Pt(2-thpy)$_2$ in *n*-octane at $T = 1.3$ K, with detection at 16 444 cm^{-1} (I-713 and I-718 cm^{-1} emission satellites; see also the caption to Figure 7). The spectrum shows the spectral region of a higher lying state, presumably of MLCT character (see also ref 65). The spectra are normalized to the peak at 20 430 cm^{-1}.

of state $|\mathrm{I}\rangle$ τ_I is 230 μs (Figure 9). (In this case, a consideration of the emission lifetime τ_II, as in eq 3, is not necessary, since the correction would be smaller than the experimental error of $\pm$5 ns.) Similar to the situation for Pt(2-thpy)$_2$, the mechanism of slr at low temperature was assigned to a direct process.[49] Again, this can be deduced from the very weak temperature dependence of T_1 up to $T \approx 6$ K.[50] However, with further temperature increase—as could be shown in the recent study[50]—the slr rate grows in rapidly and is then dominated by an Orbach process with an activation energy of $\Delta = 52$ cm^{-1} (eq 2). This energy corresponds well to the separation between states $|\mathrm{II}\rangle$ and $|\mathrm{III}\rangle$ (Figure 9).

(73) In the early study[49] we reported a value for T_1 of 180 ns. Because of the better time resolution now available, we are able to correct this decay time to 220 ns.

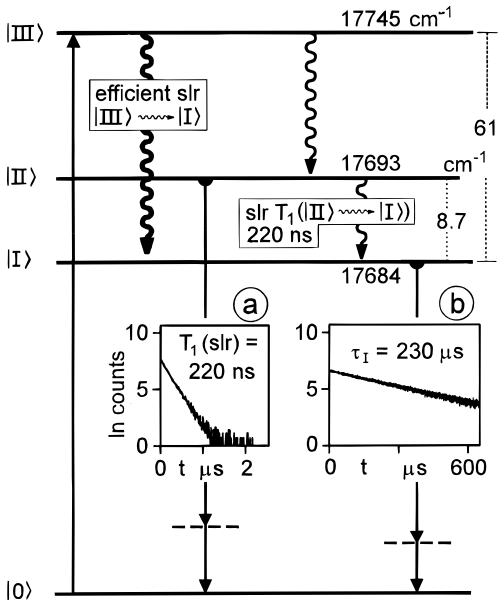

Figure 9. Energy level diagram and spin−lattice relaxation properties for the three lowest triplet sublevels of $[Ru(bpy)_3]^{2+}$ doped into $[Zn(bpy)_3](ClO_4)_2$ ($T = 1.3$ K). The emission from the higher lying state $|\mathrm{II}\rangle$ cannot be frozen out according to a relatively slow slr from $|\mathrm{II}\rangle$ to $|\mathrm{I}\rangle$. Thus, an emission from $|\mathrm{II}\rangle$ may be registered within the first several hundred nanoseconds after an excitation pulse. Subsequently, the compound emits with its usual low-temperature emission lifetime of $\tau_\mathrm{I} = 230$ μs from state $|\mathrm{I}\rangle$.

According to this slow relaxation from state $|\mathrm{II}\rangle$ to state $|\mathrm{I}\rangle$, the emission from $|\mathrm{II}\rangle$ cannot be frozen out even at $T = 1.3$ K. Thus, one can separate the two emissions by time-resolved emission spectroscopy. The spectrum measured during the first 300 ns after the laser pulse represents (mainly) the emission from state $|\mathrm{II}\rangle$, while the emission from state $|\mathrm{I}\rangle$ is registered, for example, with a delay of $t = 10$ μs and a time window of

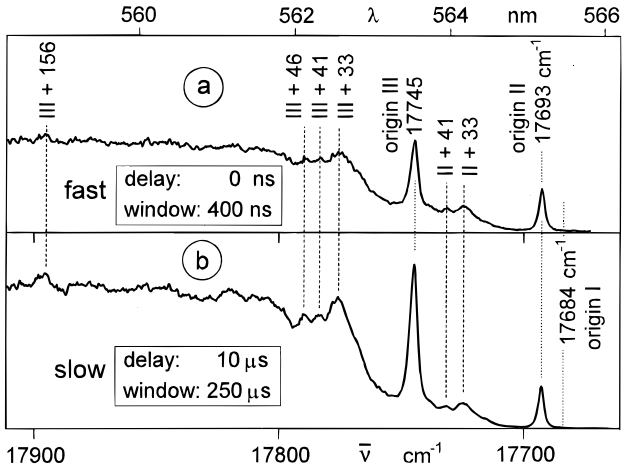

Figure 10. Time-resolved excitation spectra of $[Ru(bpy)_3]^{2+}$ doped into $[Zn(bpy)_3](ClO_4)_2$ ($T = 1.3$ K). The emission is detected at $\bar{\nu}_{det} = 17\,037$ cm^{-1}, where the short-lived emission from state $|II\rangle$ and the long-lived one from $|I\rangle$ overlap. The spectra are normalized to the origin II peaks. Excitation peak III is more intense in the slow spectrum (b) compared to the fast one (a) due to the more efficient spin−lattice relaxation from state $|III\rangle$ to state $|I\rangle$ than from $|III\rangle$ to $|II\rangle$. (See also Figure 9.) Note that origin I is not observed in excitation spectra because of the extremely small probability of transition from the ground state $|0\rangle$ to state $|I\rangle$ (see, for example, refs 29 and 75).

$\Delta t = 200$ μs. These spectra, not reproduced here (but see refs 29, 49, and 69), are distinctly different, and it is found that a series of vibrational satellites belong selectively to the state $|I\rangle$ and others to the state $|II\rangle$ emission. Thus, one observes a shift of the whole spectrum with time. It is emphasized that this spectral shift has nothing to do with a localization process, as assumed in ref 73. It is simply a consequence of the slow relaxation (slr) from state $|II\rangle$ to state $|I\rangle$ and different vibrational coupling properties of both states.[29,50]

3.3.2. Time-Resolved Excitation Spectra and Relaxation Paths. At low temperature, a selective excitation of state $|III\rangle$ should exhibit a distinctly more efficient slr to state $|I\rangle$ compared to state $|II\rangle$, since in both cases the slr will be dominated by direct processes, which are governed by the $(\Delta E)^3$ dependence (eq 1). Because state $|I\rangle$ exhibits a very long 230 μs decay, while state $|II\rangle$ shows a short-lived decay of 220 ns, it is expected that a pulsed excitation into state $|III\rangle$ gives a larger signal in the long-time range (from state $|I\rangle$) than in the short-time emission (form state $|II\rangle$). On the other hand, a selective excitation into state $|II\rangle$ will mainly exhibit a short-lived state $|II\rangle$ emission, since the relaxation to state $|I\rangle$ is "hindered" because of the slow slr. This situation provides a suitable basis for an application of time-resolved excitation spectroscopy. A similar situation has been described in section 3.2.3 for $Pt(2\text{-thpy})_2$.

Figure 10 displays the time-resolved excitation spectra for $[Ru(bpy)_3]^{2+}$ measured at $T = 1.3$ K. The vibrational satellite structure could spectrally only be resolved for the energy range up to $\approx$160 cm^{-1}. Figure 10b shows the slow emission. It is detected after a delay of $t = 10$ μs and thus results only from the long-lived state $|I\rangle$. The fast spectrum ($t = 0$ ns, $\Delta t = 400$ ns, Figure 10a) stems nearly exclusively from state $|II\rangle$. For a better comparison, both spectra are normalized to the excitation intensity of origin II. Interestingly, the spectra clearly display the predictions. The excitation intensity of origin III is larger by a factor of about 2.1 in the slow spectrum than in the fast one. It is Important that the *same factor* (within $\approx\pm$10%) is displayed in the range of the phonon satellites and the 156 cm^{-1} vibrational satellite. Consequently, it may be concluded that at least up to this energy of $\approx$160 cm^{-1} the relaxation occurs within the individual potential hypersurface of triplet sublevel $|II\rangle$ and $|III\rangle$, respectively.

For completeness, it is pointed out that the times of spin−lattice relaxation at $T = 1.3$ K from states $|II\rangle$ to $|I\rangle$ of $Pt(2\text{-thpy})_2$ (700 ns) and of $[Ru(bpy)_3]^{2+}$ (220 ns) differ distinctly, although for both compounds the relaxation is ascribed to a direct process of slr. Even if the difference in energy separations of $\Delta E = 7$ and 8.7 cm^{-1}, respectively, is taken into account (eq 1), the relaxation rate is still distinctly larger for $[Ru(bpy)_3]^{2+}$ than for $Pt(2\text{-thpy})_2$. This behavior is not unexpected, since $Pt(2\text{-thpy})_2$ in a Shpol'skii matrix exhibits a smaller coupling to the environment than $[Ru(bpy)_3]^{2+}$ in the $[Zn(bpy)_3](ClO_4)_2$ matrix. This is, for example, displayed in the relative intensities of the phonon satellites observed in the corresponding emission spectra. (Compare Figures 7 and 10.) However, the velocities of sound, entering in the fifth power into eq 1, should not be disregarded. Unfortunately, the values for the corresponding matrices are not yet known.

4. Conclusion

The lowest excited states of transition metal complexes are often not in a fast thermal equilibrium according to relatively slow spin−lattice relaxations (slr) at low temperatures (e.g., $T = 1.3$ K). Thus, after an excitation, these states, representing for example different triplet sublevels, emit independently, usually with different emission lifetimes, but the spectra are superimposed. However, they can often be separated from each other by time-resolved emission measurements. From these time-resolved spectra, one obtains a deeper insight into specific, still not well-known vibronic couplings of the individual electronic states. Moreover, at energy separations ΔE of several cm^{-1} between the lowest excited states and at $T = 1.3$ K, the slr are dominated by direct processes. The corresponding rates depend strongly on these energy separations ($\sim(\Delta E)^3$). Thus, those relaxation paths with larger ΔE values are preferred. Importantly, this preference is clearly displayed in the emission intensities. Consequently, an emission resulting from a specific state (exhibiting a defined decay time) can carry information about the individual relaxation path which populates that specific state from a higher lying state. It is a highlight of the present investigation that this property has been used for the first time to study details of relaxation paths in the mainfold of excited states by introducing the new method of time-resolved excitation spectroscopy. This method complements investigations of subpicosecond time resolution.

The new method of time-resolved excitation spectroscopy described in the present investigation seems to be applicable to many transition metal complexes and has been successfully applied here to $Pt(2\text{-thpy})_2$ and $[Ru(bpy)_3]^{2+}$. In particular, it has been shown that the relaxations from higher lying vibrational states occur by very fast processes (compared to spin−lattice relaxations) *within* the individual potential hypersurface of each triplet sublevel. An inter-sublevel system crossing occurs subsequently, after the respective zero-point vibrational level is reached. (A spin-flip is usually slower than the process of internal conversion.) Moreover, it was shown that this method could very usefully be applied to assigning important and often unknown correlations between electronic sublevels and vibrational excitation satellites, which are usually superimposed in time-integrated spectra.

Acknowledgment. Financial support by the Deutsche Forschungsgemeinschaft and the Verband der Chemischen Industrie is gratefully acknowledged. We also thank Degussa AG (Hanau, Germany) for donations of $RuCl_3 \cdot H_2O$ and $K_2[PtCl_4]$.
IC960565P

(74) Ferguson, J.; Krausz, E. *Chem. Phys.* **1987**, *112*, 271.
(75) Yersin, H.; Braun, D.; Hensler, G.; Gallhuber, E. In *Vibronic Processes in Inorganic Chemistry*; Flint, C. D., Ed.; Kluwer Academic Publishers: Dordrecht, The Netherlands, 1989; p 195.